Dynamical Cooper pairing in non-equilibrium electron-phonon systems

Michael Knap,[1] Mehrtash Babadi,[2] Gil Refael,[2] Ivar Martin,[3] and Eugene Demler[4]

[1]*Department of Physics, Walter Schottky Institute, and Institute for Advanced Study,*
Technical University of Munich, 85748 Garching, Germany
[2]*Institute for Quantum Information and Matter, Caltech, Pasadena, CA 91125, USA*
[3]*Materials Science Division, Argonne National Laboratory, Argonne, IL 60439, USA*
[4]*Department of Physics, Harvard University, Cambridge MA 02138, USA*
(Dated: January 26, 2016)

Ultrafast laser pulses have been used to manipulate complex quantum materials and to induce dynamical phase transitions. One of the most striking examples is the transient enhancement of superconductivity in several classes of materials upon irradiation with high intensity pulses of terahertz light. Motivated by these experiments, we analyze the Cooper pairing instabilities in non-equilibrium electron-phonon systems. We demonstrate that the light induced non-equilibrium state of phonons results in a simultaneous increase of the superconducting coupling constant and the electron scattering. We analyze the competition between these effects and show that the dynamic enhancement of Cooper pair formation dominates over the increased scattering rate in a broad range of parameters. This opens the possibility of transient light induced superconductivity at temperatures considerably higher than the equilibrium transition temperatures. Our results pave new pathways for engineering high-temperature light-induced superconducting states.

Manipulating and controlling material properties with light pulses offers exciting perspectives not only for fundamental sciences but also for technological applications [1, 2]. In ultrafast pump-probe spectroscopy, the sample is irradiated with a short pump pulse of high intensity, thereby driving the system out of equilibrium. The changes in the material are subsequently measured by a probe pulse at well defined delay times. Applying such techniques to strongly correlated systems has made it possible to transform them from one phase to another. For instance, long-range charge density wave order has been melted by light [3–6], insulators have been destroyed [7–9], and the breaking of superconducting pairs has been observed [10–14]. Remarkably, in contrast to destroying long-range order, the dynamic emergence of transient spin-density wave [15], charge-density wave [16], as well as superconducting order [17–21] has been demonstrated by resonantly exciting samples with light. This opens many theoretical questions on the origin of the light induced order, including: What is the mechanism for the emergence of transient collective behavior? What determines the lifetime of transient ordered states? How robust and universal are the observed phenomena? Answers to these questions may hold the key to a novel route for achieving ordered many-body states by periodic driving as opposed to cooling; a subject that has attracted considerable theoretical attention [22–28].

Here, we propose a mechanism for making a normal conducting metal unstable toward Cooper-pair formation by irradiation with light. Our qualitative arguments are as follows (Fig. 1): The pump pulse couples coherently to infrared-active phonon modes at zero momentum which in turn via nonlinear phonon interactions drive Raman phonon modes that are responsible for superconductivity. Depending on the form of the nonlinearity (see Tab. I for their classification) different effects can arise, including

the renormalization of the parameters of an effectively *static* Hamiltonian, the *dynamic* excitation of phonons over a broad range of momenta into squeezed states, and the *periodic* modulation of system parameters leading to Floquet states. In this work, we focus on an experimentally relevant phonon nonlinearity that hosts all of these effects. The static renormalization of the system parameters can, depending on material-specific details, either enhance or suppress the superconducting coupling constant, and hence either enhance or decrease the transition temperature T_c toward a paired state. By contrast, phonon squeezing universally suppresses the effective electronic bandwidth, and thus increases the density of states at the Fermi level, corresponding to a *universal* increase of the superconducting coupling constant. Squeezed states of phonons have also been studied in the context of optomechanical systems as a mechanism to enhance nonlinear couplings [29]. Furthermore, the periodic modulation of the system parameters can enhance Cooper pairing via a superconducting proximity effect in time rather than space.

The non-equilibrium occupation of phonons also increases the electron scattering rate which leads to Cooper pair breaking. We analyze the competition between the enhanced Cooper pair formation and Cooper pair breaking processes and show that the enhancement of pairing can dominate in a broad range of parameters resulting in signatures of superconductivity that appear at higher temperatures compared to equilibrium. We note that the predicted enhancement of T_c should be understood as a transient phenomenon, since inelastic scattering of electrons with excited phonons will eventually heat the system and destroy the superconducting order. Although our study is motivated by specific experiments, our goal here is to introduce minimal electron-phonon models which describe the origin of these effects in order to elucidate the main physical principles rather than pro-
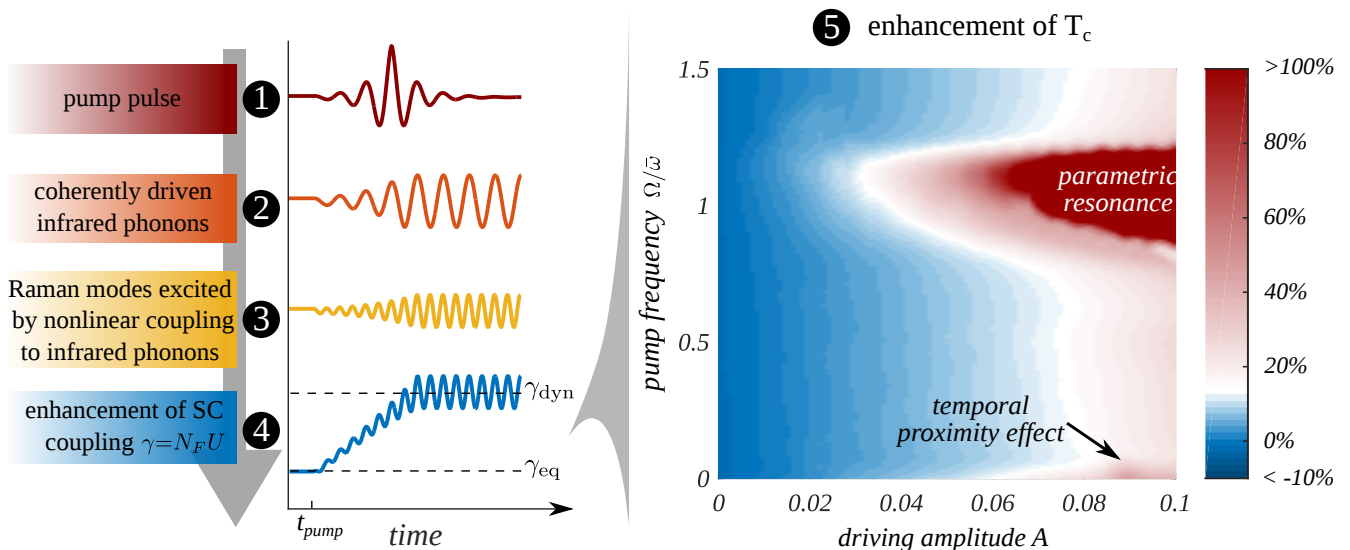
FIG. 1. **Dynamical enhancement of the superconducting transition temperature.** A schematic representation of the physical processes leading to light-induced superconductivity: (1) The pump pulse couples coherently to (2) an infrared-active phonon mode which in turn (3) via nonlinear interactions drives Raman phonons that are responsible for superconducting pairing. The non-equilibrium occupation of the Raman phonons (4) universally enhances the superconducting coupling strength γ, which is a product of the density of states at the Fermi level N_F and the induced attractive interaction between the electrons U, and hence (5) increases the transition temperature T_c of the superconducting state. We calculate the relative enhancement of T_c compared to the equilibrium $T_{c,eq}$ by taking into account the competition between dynamical Cooper pair-formation and Cooper pair-breaking processes, as a function of the pump frequency $\Omega/\bar\omega$ and the driving amplitude A. The data is evaluated for linearly dispersing phonons with mean frequency $\bar\omega$, relative spread $\Delta\omega/\bar\omega = 0.2$, and negative quartic couplings of type II between the Raman and infrared active modes, *cf.* Tab. I. Moreover, the electron-phonon interaction strength is chosen to give an equilibrium effective attractive interaction $U/W = 1/8$ that is weak compared to the bare electronic bandwidth W. The static renormalization of Raman modes leads to the uniform increase of T_c with increasing driving amplitude A, the squeezed phonon state manifests in the strong enhancement near parametric resonance $\Omega \sim \bar\omega$, and the temporal proximity effect dominates near $\Omega/\bar\omega \sim 0$.

viding detailed material-specific *ab initio* computations.

While our main focus in this work is on superconducting instabilities, the proposed mechanism can be readily applied to other types of long-range order such as charge-density wave or spin-density wave order, by performing the instability analysis in the respective channels.

I. ROLE OF THE PHONON NONLINEARITY

Strong terahertz-frequency pulses can resonantly drive infrared-active phonon modes which have a finite dipole

TABLE I. **Types of the phonon nonlinearities and their static and non-equilibrium effects on the system.** The renormalization of the parameters leads to an effectively static Hamiltonian, while phonon squeezing and the periodic Floquet modulation of system parameters are purely dynamical.

	static renorm. of parameters	dynamical squeezing	periodic Floquet
I: $(Q_0^{IR})^2 Q_0^R$	✓	✗	✓
II: $(Q_0^{IR})^2 Q_k^R Q_{-k}^R$	✓	✓	✓
III: $Q_0^{IR} Q_k^R Q_{-k}^R$	✗	✓	✓

moment, see Fig. 1. The high-intensity pump pulse has a momentum that is negligible compared to the reciprocal lattice vector. The drive thus creates a coherent phonon state at zero momentum, $Q_{q=0}^{IR}(t) = E\cos\Omega t$, where Ω is the drive frequency and E is proportional to the pulse amplitude. In the presence of phonon nonlinearities, the driven infrared-active phonon mode couples to Raman modes Q_q^R of the crystal [18, 22, 30, 31] which in turn can couple to the conduction electrons. In this section, we discuss the three leading types of phonon nonlinearities, *cf.* Tab. I and characterize their static and dynamic effects. A static renormalization of the Hamiltonian parameters arises from phonon nonlinearities that involve even powers of Q_0^{IR}. Since these terms have finite time averages, the static (time-averaged) Hamiltonian will be modified. For phonon nonlinearities of type I (see Tab. I), this term leads to a static displacement of the zero-momentum Raman phonon. For nonlinearities of type II, however, the frequency of the Raman phonons is modified. In both cases we expect strong effects on the superconducting instability which can be analyzed following the standard Migdal-Eliashberg formalism [32]. In this paper our focus will mostly be on the effects of the dynamical (oscillatory) part of the drive on super-

conductivity. These effects can be divided into two contributions: First, the system parameters will generically oscillate in time due to the drive. Second, nonlinearities that couple to finite momentum Raman modes $Q_k^R Q_{-k}^R$, as in case II and III, dynamically squeeze the phonons. In the following, we discuss the different classes of phonon nonlinearities in more detail.

A. Type I nonlinearity: Uniform lattice displacement

A nonlinear phonon coupling of form I: $\Lambda(Q_0^{IR})^2 Q_0^R$ acts as a classical force on Q_0^R proportional to $(Q_0^{IR})^2$ [18, 22, 30, 31]. The drive $(Q_0^{IR})^2 = E^2 \cos^2 \Omega t = \frac{E^2}{2}(1 + \cos 2\Omega t)$ can be separated in a static and an oscillatory contribution. Taking a simple electron-phonon model in which the phonons modulate electron hopping processes $-(J_0 + g Q_0^R) \sum_{\langle ij \rangle, \sigma} c_{i\sigma}^\dagger c_{j\sigma}$ (g is the electron-phonon coupling and $c_{i\sigma}^\dagger$ the electron creation operator) as for example in a Su-Schrieffer-Heeger (SSH) model [33], the finite displacement of the lattice along the coordinates of the Raman mode renormalizes the electron tunneling by a term $\propto g\Lambda E^2$, see Supplementary Information (SI). The effective electronic bandwidth is reduced when $g\Lambda < 0$; a condition that is material specific. Reducing the bandwidth results in a higher density of states and hence an enhanced superconducting transition temperature T_c. For $g\Lambda > 0$ contrary is the case. These general considerations may account for the physical origin of the enhancement of the transition temperature which has been seen in *ab initio* calculations for specific materials [18]. On top of the enhancement due to the time-averaged displacement of the Raman phonon mode, the strong oscillations at 2Ω can give rise to an additional dynamic enhancement of T_c by the temporal proximity effect as as we discuss later in this work.

B. Type II and III nonlinearities: Finite-momentum phonon excitations

Another type of phonon nonlinearities in centro-symmetric crystals is the quartic form $\Lambda_k(Q_0^{IR})^2 Q_k^R Q_{-k}^R$ (type II). In this case, the coherently driven infrared phonon excites Raman phonons in pairs and with opposite finite momenta, leading to quantum correlations between k and $-k$ modes. These states are referred to as *squeezed states* in quantum optics [34]. The drive can be again separated into a static and an oscillatory term with the implications of the static displacement being crucially dependent on the sign of the nonlinearity Λ_k. For $\Lambda_k < 0$ the frequencies of the Raman modes ω_k are softened and hence the effective electron-electron interaction, which is typically of the form g_k^2/ω_k, is increased, while for $\Lambda_k > 0$ the opposite is the case. By contrast, we find that irrespective of the sign of the couplings, the

oscillatory term squeezes the Raman modes which results in a polaronic suppression of the electron tunneling matrix element compared to equilibrium and hence in an enhanced density of states. Such an enhancement in the density of states in turn increase the superconducting coupling constant, enabling dynamic Cooper pair formation at higher temperatures where equilibrium Cooper pairing would be impossible.

In non-centrosymmetric crystals, the lowest order phonon nonlinearity is of the cubic form III: $Q_0^{IR} Q_k^R Q_{-k}^R$, which gives rise to phonon squeezing that leads to an enhanced T_c. Therefore, the effect of phonon squeezing is largely insensitive to the microscopic details of the phonon nonlinearities.

In the remainder of this work we will focus on the type II nonlinearity as it covers the static renormalization of the Hamiltonian parameters, dynamical phonon squeezing, and the periodic modulation. Moreover, it is relevant to recent experiments on fulleride superconductors [21]. Further discussions regarding type I and type II nonlinearities are provided in the SI.

II. A MINIMAL ELECTRON-PHONON MODEL

We illustrate the aforementioned effects in detail using a minimal model with Fröhlich-type electron-phonon interactions that couple the displacement of the Raman phonons Q_k^R to the local electron density $n_{i\sigma}$:

$$\hat{H}_{\text{el-ph}} = -J_0 \sum_{\langle ij \rangle, \sigma} c_{i\sigma}^\dagger c_{j\sigma} + \sum_k (P_k^R P_{-k}^R + \omega_k^2 Q_k^R Q_{-k}^R)$$
$$+ \sum_{ik\sigma} \sqrt{\frac{2\omega_k}{V}} g_k e^{ikr_i} Q_k^R n_{i\sigma}. \quad (1)$$

In this work, we consider dispersive optical phonons with mean frequency $\bar{\omega}$ and spread $\Delta\omega$. With the aforementioned quartic nonlinearities of type II, the phonon drive term, introduced for $t > 0$, reads

$$\hat{H}_{\text{drv}}(t) = -\sum_k \omega_k^2 A_k(1 + \cos 2\Omega t)Q_k^R Q_{-k}^R, \quad (2)$$

where $A_k = -\Lambda_k E^2 / 2\omega_k^2$ and E is the amplitude of the driven infrared active phonon.

In equilibrium, the electron tunneling is suppressed by polaronic dressing. Upon hopping on the lattice, the electron distorts it and drags phonons. For such a dressed tunneling process of the electron, the matrix element is suppressed by the Franck-Condon overlap of the shifted and unshifted phonon modes: $J_{\text{eq}} = J_0 \exp[-g^2/\omega^2]$. Out of equilibrium we find an enhanced polaronic dressing due to the excited states of phonons. We emphasize that the effect of the drive is twofold. First, due to the static contribution, we find renormalized phonon frequencies, which for negative nonlinearities, $-A_k \sim \Lambda_k < 0$, are softened by $\omega_k^2(1 - A_k)$. The mode softening suppresses the electron tunneling. Second, the time dependent part of the drive (2) realizes a parametrically driven

oscillator which dynamically generates squeezing correlations and hence further suppresses the electron tunneling matrix element. While mode softening depends on the sign of the nonlinearity, the dynamical generation of squeezing correlations is a *universal* process independent of the microscopic details.

Before discussing the details of our analysis, we qualitatively describe the approach we introduce for studying non-equilibrium superconductivity. We perform the Lang-Firsov transformation (*cf.* Methods), which eliminates the electron-phonon interaction term in equation (1) but introduces an effective electron-electron interaction and dresses the electron tunneling with phonons. This dressing, which depends on the phonon squeezing, suppresses the electron tunneling and modulates it in time.

Our general strategy is to (i) take into account the softening of the Raman modes by a static renormalization of the phonon coordinates and (ii) treat the dynamic excitation of finite-momentum phonons generated by the drive by transforming the system into a rotating frame in which the initial phonon distribution remains constant at all times (*cf.* Methods). Since we are considering optical phonons, we assume their thermal occupation to be negligible before the drive was switched on. Taking the phonon expectation value leads to the dressed electron tunneling matrix element $\hat{H}_{\rm kin} \to J(t) \sum_{ij\sigma} c_{i\sigma}^\dagger c_{j\sigma}$. (iii) We compute the rate of non-equilibrium Cooper pair breaking processes resulting from dynamical excitations of the Fermi sea induced by the drive and take into account the competition between the enhanced pair formation and pair breaking. This treatment is justified by showing *a posteriori* that pair breaking is subdominant compared to pair formation.

Solving the full problem numerically (SI) we find that $J(t)$ oscillates with twice the driving frequency 2Ω around its mean value

$$\langle J(t)\rangle = J_{\rm eq} e^{-\zeta}, \tag{3}$$

which is suppressed by mode softening and phonon squeezing, as parametrized by ζ. Near parametric resonance the squeezing correlations increase in time leading to a decrease in $J(t)$ and an increase in the amplitude of its oscillations. Since we are studying transient phenomena, we take the average over the first ten driving cycles to extract the effective electron tunneling, *cf.* Fig. 6 in the SI. We take the electron-phonon coupling g_k such that $g_k^2/\omega_k = {\rm const.}$, which leads to a local Hubbard-type electron-electron interaction U. This assumption is reasonable for phonons with wavevectors above the Thomas-Fermi screening length [32]. We emphasize however that this assumption is not crucial for our analysis. For technical convenience, we transform the oscillatory part from the kinetic to the interaction term by rescaling time (SI),

yielding the effective time-dependent Hamiltonian

$$\tilde{H}(t) = J_{\rm eq} e^{-\zeta} \sum_{ij} c_{i\sigma}^\dagger c_{j\sigma} - U(1 + \mathcal{A}\cos 2\Omega t)\sum_i n_{i\uparrow} n_{i\downarrow}$$
$$+ \hat{H}_{\rm el\text{-}ph\ scatt.}, \tag{4}$$

where $\hat{H}_{\rm el\text{-}ph\ scatt.}$ represent electron-phonon scattering terms that vanish upon taking the phonon-vacuum expectation value in the rotating frame. The drive, equation (2), has thus several effects: (i) a suppression of the electron tunneling by a factor $\exp[-\zeta]$, (ii) a dynamic Floquet contribution from modulating the interaction energy by $\mathcal{A}\cos 2\Omega t$, and (iii) an enhancement of the electron scattering due to the non-equilibrium phonon occupation.

III. DYNAMICAL COOPER INSTABILITY

We study the dynamical Cooper instability toward pair formation in Hamiltonian (4) by combining the Bardeen-Cooper-Schrieffer (BCS) approach [35] with a Floquet analysis [36]. We also take into account the finite electron lifetime τ due to the non-equilibrium phonon occupation, by introducing an imaginary self-energy correction i/τ (calculated explicitly in the next section). In contrast to elastic scattering on a time-reversal symmetry preserving potential, where Anderson's theorem [37, 38] shows that the thermodynamics of a superconductor remains unchanged, the inelastic scattering processes arising here indeed alter the superconducting properties.

To carry out the BCS Floquet analysis of the pairing instability, we use the equations of motion technique [39]. We introduce infinitesimal pairing amplitudes $a_k = \langle c_{k\uparrow} c_{-k\downarrow}\rangle$ and determine whether the system is stable or unstable to the growth of a_k [40, 41] by finding the eigenfequencies of the corresponding collective mode. We decompose $a_k(t)$ into Floquet modes

$$a_k(t) \sim e^{-iEt} \sum_{n=-\infty}^{\infty} a_{kn} e^{2in\Omega t}, \tag{5}$$

where E is the energy which has to be determined self-consistently from the Floquet BCS gap equation (SI)

$$0 = (U^{-1} + F_n)\Delta_n + \frac{\mathcal{A}}{2} F_n(\Delta_{n-1} + \Delta_{n+1}) \tag{6a}$$

$$F_n = \frac{1}{V}\sum_k \frac{1 - 2n_k}{E + 2n\Omega - 2(\epsilon_k + i/\tau - \mu - U\rho)}. \tag{6b}$$

The instability of the system manifests itself in the appearance of an eigenmode with negative imaginary part of E which we obtain by searching for the zeros of the determinant of (6) in the complex plane of E [40, 41]. Here, $\Delta_n = \frac{U}{V}\sum_k a_{kn}^*$ are the Floquet harmonics of the gap, ρ is the electron density of a single spin-component, μ the chemical potential, n_k the Fermi-Dirac distribution of the electrons determined by the temperature of
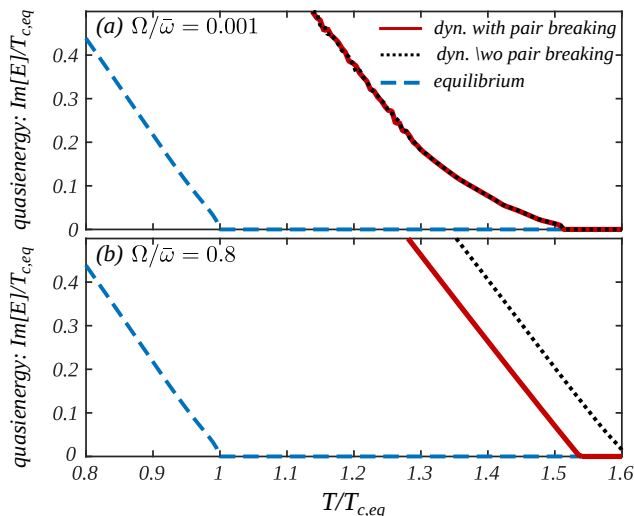
FIG. 2. **Dynamical Cooper instability.** The dynamical Cooper instability evaluated within the Floquet BCS theory *including* non-equilibrium pair-breaking processes, red solid line, is compared to the one without pair breaking, black dotted line, and the BCS solution for the equilibrium problem, blue dashed line. Data is evaluated for mean phonon frequency $\bar{\omega}/W = 1/8$ and effective attractive interactions $U/W = 1/8$ that are weak compared to the bare electronic bandwidth W, a phonon frequency spread of $\Delta\omega = 0.2\bar{\omega}$, driving strength $A = 0.1$, and driving frequency (a) $\Omega/\bar{\omega} = 0.001$ and (a) $\Omega/\bar{\omega} = 0.8$. The non-equilibrium Cooper pair formation rate dominates over the pair breaking, hence, leading to an enhanced transition temperature.

the undriven system, and ϵ_k the electron dispersion. The assumed thermal state of the electrons is justified in the weak-coupling regime and since we are only interested in transient effects that follow the drive [42]. We determine the critical T_c by locating the highest temperature at which we find an unstable solution of the Floquet BCS gap equations (6). Equations with similar structure are obtained for spatially inhomogeneous superconductors [43].

The high and low frequency limits of the BCS Floquet gap equations (6) can be understood from perturbative arguments. In the high frequency limit, $\Omega \to \infty$, we use a Magnus expansion to derive the stroboscopic Floquet Hamiltonian [36]. To zeroth order in $1/\Omega$, the Floquet Hamiltonian is given by the time averaged Hamiltonian. Thus for the harmonic drive in equation (4), the contribution $\sim \mathcal{A}$ drops out to lowest order and we obtain an equilibrium BCS gap equation with interaction U and the reduction of the electron tunneling $J_{eq} \exp[-\zeta]$ due to the squeezed phonon state. Enhancement of T_c due to the suppression of the effective electron bandwidth by radiation has also been suggested in a model without phonons [25].

In the low frequency limit $\Omega \to 0$, the core of the Floquet BCS gap equations (6) barely depends on the Flo-

quet band index n leading to

$$[U^{-1} + F(1 + \mathcal{A})]\Delta = 0. \tag{7}$$

The maximally enhanced transition temperature T_c is thus determined by an equilibrium BCS gap equation with $U(1 + \mathcal{A})$ which is the largest instantaneous attractive interaction. Hence, in the slow drive limit, the pairing induced by the strongest instantaneous interaction dominates the Cooper pair formation which can be interpreted as a superconducting proximity effect in time rather than in space.

We confirm these perturbative predictions by numerically solving the Floquet BCS gap equations (6) on a two-dimensional square lattice away from half-filling. The convergence of the results with system size and number of Floquet bands is checked. We choose linearly dispersive phonons with mean frequency $\bar{\omega}/W = 1/8$, interaction energy $U/W = 1/8$ weak compared to the bare electron bandwidth W, and set the width of the phonon branch to $\Delta\omega = 0.2\bar{\omega}$; a typical value for optical phonons. We first solve the driven phonon problem from which we determine the average suppression of the electron tunneling $e^{-\zeta}$ and the effective amplitude $\mathcal{A}$ of the oscillations in the interaction. Then we solve the Floquet BCS problem. In Fig. 2 we show the dynamical Cooper instability including pair-breaking processes for driving $\Omega/\bar{\omega} = \{0.001, 0.8\}$ and $A_k = A = 0.1$ constant for all k, red solid line, and compare them to the instability without pair breaking, black dotted line, and the equilibrium solution, blue dashed line. The reduction of the superconducting transition temperature due to the finite electron lifetime is of the Abrikosov-Gorkov form $T_c = T_{c,0} - 1/\tau$, where T_c is the dynamical transition temperature including pair-breaking and $T_{c,0}$ the one without pair breaking. We find an enhancement of the dynamical transition temperature T_c compared to equilibrium, see Fig. 2, and hence that the pair formation rate dominates the pair-breaking rate. In the high-frequency limit $\Omega/\bar{\omega} = 0.8$, (b), the enhancement results mainly from the efficient suppression of the electron tunneling near parametric resonance $\Omega \sim \bar{\omega}$ and in the slow drive limit $\Omega \to 0$, (a), from a combination of mode softening and the temporal proximity effect. The relative enhancement of T_c, taking into account pair breaking processes, is shown in Fig. 1 for an extended range of driving amplitudes A and driving frequencies $\Omega/\bar{\omega}$. In summary, the enhancement displays an intricate non-monotonic dependence on the driving frequency.

IV. DYNAMICAL COOPER PAIR BREAKING

Fluctuations around the initial phonon state and the temporal modulation of the interactions *reduce* the quasiparticle lifetime which in turn decrease the superconducting transition temperature.

We compute the quasiparticle scattering rate from the phonon fluctuations $1/\tau_{ph}$ and the modulated interac-
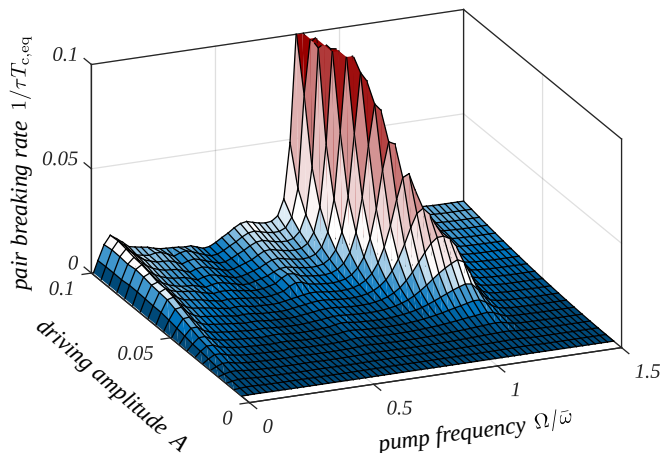
FIG. 3. **Cooper pair breaking rate**. The Cooper pair breaking rate due to phonon fluctuations and the modulation of the effective electron-electron interactions evaluated from Floquet Fermi's golden rule for $\bar{\omega} = U = W/8$.

tions $1/\tau_{\text{int}}$ by Floquet Fermi's Golden Rule (SI). Due to the time dependence of the coupling constants, energy required to create particle-hole excitations can be borrowed from the drive. This enhances the scattering rate compared to equilibrium. The total dynamic Cooper pair breaking rate $1/\tau = 1/\tau_{\text{ph}} + 1/\tau_{\text{int}}$ is shown in Fig. 3 for $\bar{\omega} = U = W/8$. For low driving frequencies, the pair-breaking rate is small, since only higher order Floquet harmonics can provide the required energy and the corresponding matrix elements are small. When the driving frequency is near parametric resonance with phonon pair excitations, the effective interactions and hence the decay rate increases since the drive can efficiently provide the required energy to create particle-hole excitations.

In broad regime of parameters we find that the enhanced pair formation rate dominates over the enhanced pair breaking rate, *c.f.* Fig. 1.

V. EXPERIMENTAL IMPLICATIONS

Even though we are not studying a specific material from first principles, it is illustrative to estimate the typical order of magnitude of the discussed effects for a recent experiment in which transient non-equilibrium superconductivity has been explored in K_3C_{60} fullerides using a pump-probe setting [21]. Typical energy scales in K_3C_{60} are the following [44]: bare bandwidth $W \sim 0.6$eV, intramolecular phonon frequencies $\omega \sim 0.03 - 0.2$eV, and electron-phonon coupling $U = g^2/\omega \sim 0.1$eV. Thus, the parameters we chose are representative for the K_3C_{60} system. In the experiment [21] the driving frequency Ω ranges from a tenth to a third of the bandwidth. Translating to our scenario, the main enhancement of T_c results from the renormalized Hamiltonian parameters and the time averaged suppression of the electron tunneling due to the phonon squeezing.

Our calculations suggest that the increase of the superconducting transition temperature is related to a dynamical enhancement of the effective electron mass, see Fig. 7 (a). Such a dynamical renormalization of the electronic dispersion can, for instance, be determined experimentally by time-resolved ARPES measurements, see e.g. [3, 11–13].

VI. SUMMARY AND OUTLOOK

We proposed a mechanism for the enhancement of Cooper pairing in driven electron-phonon systems using minimal models. The qualitative effects are as follows: First, phonon nonlinearities of type I and II, *cf.* Tab. I, that couple to the square of the infrared active phonon $(Q_0^{\text{IR}})^2$ generate a static renormalization of the Hamiltonian parameters, which depending on material-specific, *non-universal* properties can either enhance or suppress the density of states at the Fermi level and hence either increase or decrease T_c. Second, phonon nonlinearities of type II and III that squeeze Raman modes at finite momenta, give rise to a *universal* enhancement of the density of states due to polaronic effects and thus enhance the Cooper pair formation. Third, the periodic modulation of the microscopic parameters leads to a temporal proximity effect which at low frequencies enhances pairing. However, the non-equilibrium distribution of phonons has also to be taken into account as it enhances Cooper pair breaking. We studied the competition between the increased Cooper pair formation and Cooper pair breaking and found that the latter does not inhibit the dynamic enhancement of T_c in a broad parameter range. Even though we focused on superconducting instabilities, the proposed mechanism for achieving a larger coupling constant is generic and can be directly applied to other forms of long-range order such as spin or charge density waves.

The present analysis addresses the transient dynamics of the system. At long times, the inelastic scattering of electrons from excited phonons will increase their temperature and will tend to destroy superconducting order, as seen in the experiments. At intermediate times, heating of the electrons can give rise to nonequilibrium distribution functions which potentially enhances superconducting coherence as experimentally seen by microwave irradiation of superconducting samples [45, 46]. The analysis of complete thermalization due to feedback effects in a fully self-consistent and conserving calculation is an exciting future direction.

METHODS

We take the static Raman mode softening in equation (2) into account by renormalizing the phonon coordinates. A Lang-Firsov transformation [32] is applied to Hamiltonian (1), which removes the electron-phonon
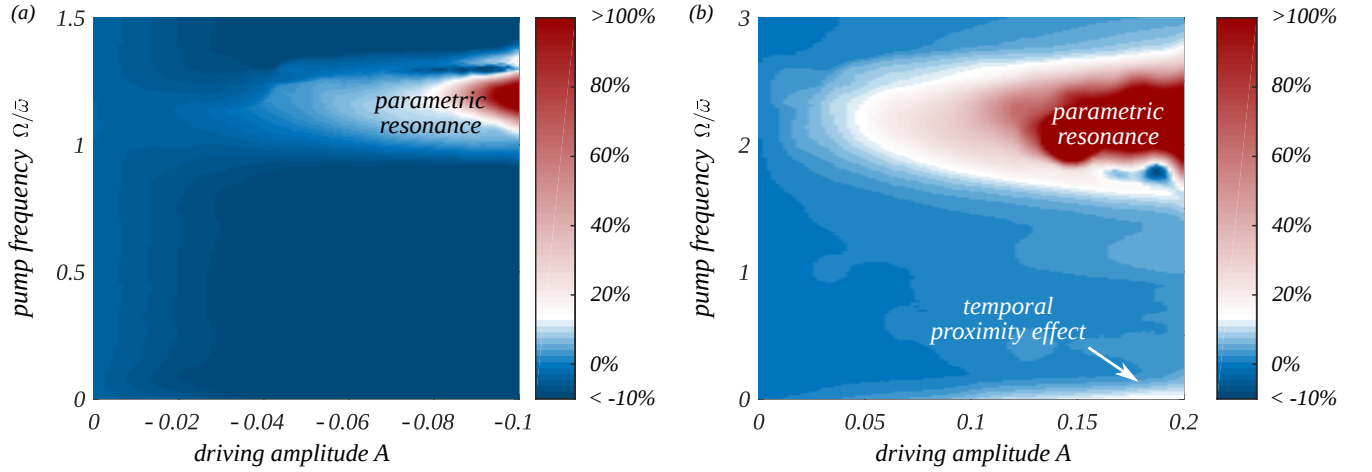
FIG. 4. **Extended data figure: Phonon squeezing as a universal mechanism for the enhancement of T_c.** The relative change of the superconducting transition temperature is shown for (a) quartic type II phonon nonlinearities with positive $\Lambda_k > 0$ and (b) cubic type III phonon nonlinearities, taking into account the competition between Cooper pair formation and pair breaking. (a) Quartic phonon nonlinearities that couple to finite momentum Raman modes have two distinguished effects on the bandwidth renormalization: (i) the static displacement of the Raman modes and (ii) phonon squeezing. For positive nonlinearities, the static displacement hardens the frequency of the Raman phonons. This leads to the uniform suppression of T_c with increasing magnitude of the driving amplitude A. However, near parametric resonance $\Omega \sim \bar{\omega}$, the phonon squeezing dominates over the static displacement, leading to the universal enhancement of T_c. (b) Cubic nonlinearities exhibit only the squeezing mechanism, and hence irrespectively of the sign of the coupling lead to an enhanced transition temperature. Furthermore, the shape of the enhancement diagram is similar to the one for quartic interaction with the main difference that in the case of quartic nonlinearities the resonance condition is $\Omega \sim \bar{\omega}$ while in the cubic case it is $\Omega \sim 2\bar{\omega}$. The data is evaluated for $\bar{\omega}/W = 1/8$, $U/W = 1/8$, $\Delta\omega = 0.2\bar{\omega}$.

interaction term, but in turn dresses the electron tunneling with the phonon displacement and introduces an attractive electron-electron interaction

$$\hat{H} = -\sum_{ij\sigma} J_{ij} c_{i\sigma}^\dagger c_{j\sigma} - \sum_{ij\sigma\sigma'} U_{ij} n_{i\sigma} n_{j\sigma'} + \hat{H}_{\text{ph}}, \quad (8)$$

where $J_{ij} = J_0 \exp[-\frac{1}{\sqrt{V}} \sum_k \frac{g_k(e^{ikr_i} - e^{ikr_j})}{\omega_k(1-A_k)^{3/4}}(b_k - b_{-k}^\dagger)]$, $U_{ij} = \frac{1}{V} \sum_k e^{-ik(r_j - r_i)} \frac{g_k^2}{\omega_k(1-A_k)^{1/2}}$, and

$$\hat{H}_{\text{ph}} = \sum_k (P_k^{\text{R}} P_{-k}^{\text{R}} + \omega_k^2 Q_k^{\text{R}} Q_{-k}^{\text{R}}) + \hat{H}_{\text{drv}} = \hat{H}_{\text{ph},0} + \hat{H}_{\text{drv}}. \quad (9)$$

The phonon Hamiltonian (9) describes a driven parametric oscillator [47] which excites a squeezed state of k and $-k$ modes. The effect is strongest on resonance, $\omega_k \sim \Omega$, where the system undergoes a parametric instability and phonon squeezing parametrized by $\xi(t)$ increases linearly in time [34] which in turn reduces the electron tunneling matrix element exponentially in time. Off-resonantly driven phonon modes will benefit from squeezing correlations as well.

We solve the problem by constructing a time dependent unitary transformation W [48] that removes the drive

$$W^\dagger(\hat{H}_{\text{ph},0} + \hat{H}_{\text{drv}})W - iW^\dagger \frac{dW}{dt} = \hat{H}_{\text{ph},0}. \quad (10)$$

Applying the unitary to the full Hamiltonian $W^\dagger \hat{H} W$ in equation (8), leaves the attractive interaction unchanged but transforms the kinetic energy to

$$\hat{H}_{\text{kin}} \to -J(t) \sum_{ij\sigma} e^{-\sum_k \alpha_k^*(t)\Gamma_k^* b_k^\dagger} e^{\sum_k \alpha_k(t)\Gamma_k b_k} c_{i\sigma}^\dagger c_{j\sigma}, \quad (11)$$

where $J(t) = J_0 \exp[-\frac{1}{V} \sum_k (1 - \cos k) \frac{g_k^2 |\alpha_k(t)|^2}{\omega_k^2(1-A_k)^{3/2}}]$ is the suppressed electron hopping, Γ_k contains information about the lattice geometry, and α_k is related to the phonon squeezing in such a way that upon taking the time average $\langle |\alpha_k(t)|^2 \rangle = \langle \cosh 2|\xi_k(t)| \rangle$ (SI). The latter contributes to the Franck-Condon suppression for squeezed states, which is smaller than the one at equilibrium $J_{\text{eq}} = J_0 \exp[-\frac{1}{V} \sum_k (1 - \cos k) \frac{g_k^2}{\omega_k^2}]$. We introduce ζ to parametrize the relative suppression of the electron tunneling compared to the one at equilibrium, see equation (3).

---

[1] Orenstein, J. Ultrafast spectroscopy of quantum materials. *Physics Today* **65**, 44–50 (2012).

[2] Zhang, J. & Averitt, R. Dynamics and Control in Complex Transition Metal Oxides. *Annu. Rev. Mater. Res.* **44**, 19–43 (2014).

[3] Schmitt, F. *et al.* Transient Electronic Structure and Melting of a Charge Density Wave in TbTe$_3$. *Science* **321**, 1649–1652 (2008).

[4] Yusupov, R. *et al.* Coherent dynamics of macroscopic electronic order through a symmetry breaking transition. *Nat. Phys.* **6**, 681–684 (2010).

[5] Hellmann, S. *et al.* Ultrafast Melting of a Charge-Density Wave in the Mott Insulator 1T - TaS$_2$. *Phys. Rev. Lett.* **105**, 187401 (2010).

[6] Rohwer, T. *et al.* Collapse of long-range charge order tracked by time-resolved photoemission at high momenta. *Nature* **471**, 490–493 (2011).

[7] Rini, M. *et al.* Control of the electronic phase of a manganite by mode-selective vibrational excitation. *Nature* **449**, 72–74 (2007).

[8] Hilton, D. J. *et al.* Enhanced Photosusceptibility near T_c for the Light-Induced Insulator-to-Metal Phase Transition in Vanadium Dioxide. *Phys. Rev. Lett.* **99**, 226401 (2007).

[9] Liu, M. *et al.* Terahertz-field-induced insulator-to-metal transition in vanadium dioxide metamaterial. *Nature* **487**, 345–348 (2012).

[10] Demsar, J. *et al.* Pair-Breaking and Superconducting State Recovery Dynamics in MgB$_2$. *Phys. Rev. Lett.* **91**, 267002 (2003).

[11] Cortés, R. *et al.* Momentum-resolved ultrafast electron dynamics in superconducting Bi$_2$Sr$_2$CaCu$_2$O$_{8+\delta}$. *Phys. Rev. Lett.* **107**, 097002 (2011).

[12] Graf, J. *et al.* Nodal quasiparticle meltdown in ultrahigh-resolution pump-probe angle-resolved photoemission. *Nat. Phys.* **7**, 805–809 (2011).

[13] Smallwood, C. L. *et al.* Tracking Cooper Pairs in a Cuprate Superconductor by Ultrafast Angle-Resolved Photoemission. *Science* **336**, 1137–1139 (2012).

[14] Matsunaga, R. *et al.* Higgs amplitude mode in the BCS superconductors Nb$_{1-x}$Ti$_x$N induced by terahertz pulse excitation. *Phys. Rev. Lett.* **111**, 057002 (2013).

[15] Kim, K. W. *et al.* Ultrafast transient generation of spin-density-wave order in the normal state of BaFe2as2 driven by coherent lattice vibrations. *Nat. Mater.* **11**, 497–501 (2012).

[16] Singer, A. *et al.* Enhancement of charge ordering by dynamic electron-phonon interaction. *arXiv:1511.08261* (2015).

[17] Fausti, D. *et al.* Light-Induced superconductivity in a stripe-ordered cuprate. *Science* **331**, 189 –191 (2011).

[18] Mankowsky, R. *et al.* Nonlinear lattice dynamics as a basis for enhanced superconductivity in YBa$_2$Cu$_3$O$_{6.5}$. *Nature* **516**, 71–73 (2014).

[19] Hu, W. *et al.* Optically enhanced coherent transport in YBa$_2$Cu$_3$O$_{6.5}$ by ultrafast redistribution of interlayer coupling. *Nat. Mater.* **13**, 705–711 (2014).

[20] Kaiser, S. *et al.* Optically induced coherent transport far above T_c in underdoped YBa$_2$Cu$_3$O$_{6+\delta}$. *Phys. Rev. B* **89**, 184516 (2014).

[21] Mitrano, M. *et al.* An optically stimulated superconducting-like phase in K$_3$C$_{60}$ far above equilibrium Tc. *arXiv:1505.04529* (2015).

[22] Subedi, A., Cavalleri, A. & Georges, A. Theory of nonlinear phononics for coherent light control of solids. *Phys. Rev. B* **89**, 220301 (2014).

[23] Kemper, A. F., Sentef, M. A., Moritz, B., Freericks, J. K. & Devereaux, T. P. Direct observation of higgs mode oscillations in the pump-probe photoemission spectra of electron-phonon mediated superconductors. *Phys. Rev. B* **92**, 224517 (2015).

[24] Goldstein, G., Aron, C. & Chamon, C. Photoinduced superconductivity in semiconductors. *Phys. Rev. B* **91**, 054517 (2015).

[25] Raines, Z. M., Stanev, V. & Galitski, V. M. Enhancement of superconductivity via periodic modulation in a three-dimensional model of cuprates. *Phys. Rev. B* **91**, 184506 (2015).

[26] Sentef, M. A., Kemper, A. F., Georges, A. & Kollath, C. Theory of light-enhanced phonon-mediated superconductivity. *arXiv:1505.07575* (2015).

[27] Orenstein, J. & Dodge, J. S. Terahertz time-domain spectroscopy of transient metallic and superconducting states. *Phys. Rev. B* **92**, 134507 (2015).

[28] Murakami, Y., Werner, P., Tsuji, N. & Aoki, H. Multiple amplitude modes in strongly-coupled phonon-mediated superconductors. *arXiv:1511.06105* (2015).

[29] Lemonde, M.-A., Didier, N. & Clerk, A. A. Enhanced nonlinear interactions in quantum optomechanics via mechanical amplification. *arXiv:1509.09238* (2015).

[30] Först, M. *et al.* Nonlinear phononics as an ultrafast route to lattice control. *Nat. Phys.* **7**, 854–856 (2011).

[31] Först, M., Mankowsky, R. & Cavalleri, A. Mode-selective control of the crystal lattice. *Acc. Chem. Res.* **48**, 380–387 (2015).

[32] Mahan, G. D. *Many Particle Physics* (Kluwer, New York, 2000), 3nd edn.

[33] Heeger, A. J., Kivelson, S., Schrieffer, J. R. & Su, W. P. Solitons in conducting polymers. *Rev. Mod. Phys.* **60**, 781–850 (1988).

[34] Walls, D. & Milburn, G. J. *Quantum Optics* (Springer, Berlin, Heidelberg, 2008).

[35] Bardeen, J., Cooper, L. N. & Schrieffer, J. R. Theory of superconductivity. *Phys. Rev.* **108**, 1175–1204 (1957).

[36] Bukov, M., D'Alessio, L. & Polkovnikov, A. Universal high-frequency behavior of periodically driven sys-

tems: from dynamical stabilization to Floquet engineering. *Adv. Phys.* **64**, 139–226 (2015).

[37] Anderson, P. W. Theory of dirty superconductors. *J. Phys. Chem. Solids* **11**, 26–30 (1959).

[38] Abrikosov, A. A. & Gor'kov, L. P. Theory of superconducting alloys. *Sov. Phys. JETP* **8**, 1090 (1959).

[39] Anderson, P. W. Random-phase approximation in the theory of superconductivity. *Phys. Rev.* **112**, 1900–1916 (1958).

[40] Abrikosov, A. A., Gor'kov, L. P. & Dzyaloshinskii, I. E. *Methods of Quantum Field Theory in Statistical Physics* (Dover Publications).

[41] Pekker, D. *et al.* Competition between pairing and ferromagnetic instabilities in ultracold fermi gases near feshbach resonances. *Phys. Rev. Lett.* **106**, 050402 (2011).

[42] Bauer, J., Babadi, M. & Demler, E. Dynamical instabilities and transient short-range order in the fermionic hubbard model. *Phys. Rev. B* **92**, 024305 (2015).

[43] Martin, I., Podolsky, D. & Kivelson, S. A. Enhancement of superconductivity by local inhomogeneities. *Phys. Rev. B* **72**, 060502 (2005).

[44] Gunnarsson, O. Superconductivity in fullerides. *Rev. Mod. Phys.* **69**, 575–606 (1997).

[45] Wyatt, A. F. G., Dmitriev, V. M., Moore, W. S. & Sheard, F. W. Microwave-enhanced critical supercurrents in constricted tin films. *Phys. Rev. Lett.* **16**, 1166–1169 (1966).

[46] Dayem, A. H. & Wiegand, J. J. Behavior of thin-film superconducting bridges in a microwave field. *Phys. Rev.* **155**, 419–428 (1967).

[47] Landau, L. D. & Lifshitz, E. M. *Mechanics* (Elsevier, 1982).

[48] Seleznyova, A. N. Unitary transformations for the time-dependent quantum oscillator. *Phys. Rev. A* **51**, 950–959 (1995).

CONTENTS

Appendix A: Type I nonlinearity: Uniform lattice displacement

An infrared active phonon Q_0^{IR}, coherently pumped at zero momentum, can couple via the nonlinearity $\Lambda(Q_0^{\mathrm{IR}})^2 Q_0^{\mathrm{R}}$ to zero-momentum Raman phonons Q_0^{R} that we assume to be responsible for superconductivity. In a model with Fröhlich type electron-phonon interactions the phonon displacement couples to the charge density, which is a globally conserved quantity. Hence, driving the zero-momentum phonon modes has no effect. A minimal model in which zero-momentum phonon excitations can lead to non-trivial dynamics, requires the coupling of the phonon displacement to the charge transfer, as it is the case in the extended SSH model [33]

$$H_{\mathrm{SSH}} = \sum_k \epsilon_k c_{k\sigma}^\dagger c_{k\sigma} + \sum_{kk'} \sqrt{2\omega_{k-k'}} g_{kk'} Q_{k-k'}^{\mathrm{R}} c_{k\sigma}^\dagger c_{k'\sigma} + \frac{1}{2}\sum_k (P_k^{\mathrm{R}} P_{-k}^{\mathrm{R}} + \omega_k^2 Q_k^{\mathrm{R}} Q_{-k}^{\mathrm{R}}) + \Lambda(Q_0^{\mathrm{IR}})^2 Q_0^{\mathrm{R}}. \tag{A1}$$

The infrared phonon is coherently driven, hence $Q_0^{\mathrm{IR}} = E\cos\Omega t$. Neglecting the feedback of the electrons on the phonons, we find for the phonon equation of motion

$$\ddot{Q}_0^{\mathrm{R}} + \omega_0^2 Q_0^{\mathrm{R}} = \frac{\Lambda E^2}{2}(1 + \cos 2\Omega t). \tag{A2}$$

This equation can be solved analytically with $Q_0^{\mathrm{R}}(t) = \tilde{Q} + \delta Q\cos 2\Omega t$, where $\tilde{Q} = \frac{\Lambda E^2}{2\omega_0^2}$ and $\delta Q = \frac{\Lambda E^2}{2(\omega_0^2 - 4\Omega^2)}$. The phonon displacement thus oscillates with twice the pump frequency 2Ω around a mean value $\tilde{Q}$. Plugging this into the SSH Hamiltonian, we find

$$H_{\mathrm{SSH}} = \sum_k [\epsilon_k + \sqrt{2\omega_0} g_{kk}(\tilde{Q} + \delta Q\cos 2\Omega t)] c_{k\sigma}^\dagger c_{k\sigma} + \sum_{k,q\neq 0} \sqrt{2\omega_q} g_{kk-q} Q_q^{\mathrm{R}} c_{k\sigma}^\dagger c_{k-q\sigma} + \frac{1}{2}\sum_{k\neq 0}(P_k^{\mathrm{R}} P_{-k}^{\mathrm{R}} + \omega_k^2 Q_k^{\mathrm{R}} Q_{-k}^{\mathrm{R}}). \tag{A3}$$

The Fermi velocity can be reduced by the shift due to the Raman phonon, provided $\Lambda \frac{dg_{kk}}{dk}|_{k=k_F} < 0$ which depends on the microscopic details of the system. A reduced Fermi velocity leads to an enhancement of the density of states at the Fermi level and hence to an enhancement of T_c. The effective attractive electron-electron interaction is obtained by integrating out the $k \neq 0$ phonons. As discussed in the main text, in addition to the time-averaged enhancement of the superconducting coupling constant, the transition temperature can also increase by the periodic modulation of the electron tunneling provided that the oscillation frequency is not too high.

Appendix B: Type II and III nonlinearities: Finite-momentum phonon excitations

An alternative generic mechanism for the enhancement of T_c arises when the nonlinear phonon interaction couples to pairs of Raman phonons at finite but opposite momenta. Here, we consider both the quartic type II and the cubic type III nonlinearities (see Tab. I in the main text for their classification):

Type II: Quartic nonlinearities.—For quartic nonlinearities of the form $\Lambda_k (Q_0^{\mathrm{IR}})^2 Q_{-k}^{\mathrm{R}} Q_k^{\mathrm{R}}$, the driven phonon Hamiltonian has the form

$$\hat{H}_{\mathrm{ph}} = \sum_k (P_k^{\mathrm{R}} P_{-k}^{\mathrm{R}} + \omega_k^2 Q_k^{\mathrm{R}} Q_{-k}^{\mathrm{R}}) - \sum_k \omega_k^2 A_k (1 + \cos 2\Omega t) Q_k^{\mathrm{R}} Q_{-k}^{\mathrm{R}} = \hat{H}_{\mathrm{ph},0} + \hat{H}_{\mathrm{drv.}}, \tag{B1}$$

with $A_k = -\Lambda_k E^2/2\omega_k^2$, which describes a parametric oscillator with resonance condition $\Omega = \omega_k \sqrt{1 - A_k}$. In addition to the dynamic enhancement of squeezing due to the parametric resonance which is a universal effect, the frequency of the phonon modes can be softened provided the nonlinearity is attractive $\Lambda_k < 0$, as $\omega_k \sqrt{1 - A_k} = \omega_k \sqrt{1 + \Lambda_k E^2/2} < \omega_k$ which enhances the density of states as well.

Type III: Cubic nonlinearities.—For non-centrosymmetric crystals, the zero-momentum infrared active phonon mode can directly couple to the displacement of the Raman modes $\Lambda_k Q_0^{\mathrm{IR}} Q_{-k}^{\mathrm{R}} Q_k^{\mathrm{R}}$. The effective phonon Hamiltonian arising from such a nonlinearity is

$$\hat{H}_{\mathrm{ph}} = \sum_k P_k^{\mathrm{R}} P_{-k}^{\mathrm{R}} + \omega_k^2 (1 + A_k \cos \Omega t) Q_k^{\mathrm{R}} Q_{-k}^{\mathrm{R}}, \tag{B2}$$

with $A_k = \Lambda_k E$, which also describes a parametric oscillator but with resonance condition $\Omega = 2\omega_k$. In the case of cubic interactions, direct mode softening cannot occur because the the time average of Q_0^{IR} vanishes. Nonetheless, the dynamic generation of squeezing near the parametric resonance is universally present also for cubic nonlinearities and qualitatively similar enhancement diagrams can be also obtained in that case, *cf.* Fig. 4 (b).

For phonon nonlinearities which generate squeezed states, we consider the simplest possible model giving rise to dynamics, which is the Holstein model with Fröhlich electron-phonon interactions where the phonon displacement couples to the charge density

$$H_{\mathrm{el-ph}} = -J_0 \sum_{ij\sigma} c_{i\sigma}^{\dagger} c_{j\sigma} + \sum_k \omega_k b_k^{\dagger} b_k + \frac{1}{\sqrt{V}} \sum_{ik} g_k (b_k + b_{-k}^{\dagger}) e^{ikr_i} n_{i\sigma}. \tag{B3}$$

The Holstein model exhibits nontrivial dynamics for finite-momentum phonon excitations which are not conserved. Similar results are expected for the SSH model as well.

We pursue the following strategy:

1. Using a Lang-Firsov transformation we remove the electron-phonon interaction.

2. We determine the unitary transformation W, equation (10), that transforms the system into a rotating frame in which the phonon driving is absent. This leads to a driven Floquet BCS problem.

3. We estimate the dynamic Cooper pair breaking rate due to the non-equilibrium scattering of phonons and due to oscillations in the microscopic interaction parameter using Floquet Fermi's Golden rule. The Cooper pair-breaking rate is self-consistently taken into account by adding an imaginary self-energy correction to the Floquet BCS equations.

4. Solving the driven Floquet BCS problem, we determine the enhancement of T_c relatively to the undriven one.

1. Lang-Firsov transformation

Considering the Holstein model (B3), we introduce operators $\tilde{b}_k$ and $\tilde{b}^\dagger_{-k}$ which diagonalize the static phonon Hamiltonian $\sum_k P^R_k P^R_{-k} + \omega_k^2(1 - A_k)Q^R_k Q^R_{-k}$. These operators are related to the b_k, $b^\dagger_{-k}$ operators which diagonalize $H_{\text{ph},0}$ e.g. by $(b^\dagger_{-k} - b_k) = (1 - A_q)^{\frac{1}{4}}(\tilde{b}^\dagger_{-k} - \tilde{b}_k)$. The electron-phonon interaction in equation (B3) can be removed by a Lang-Firsov transformation [32]

$$H_{\text{el-ph}} \to e^S H_{\text{el-ph}} e^{-S} \qquad \text{with} \qquad S = -\frac{1}{\sqrt{V}} \sum_{qj\sigma} \frac{g_q}{\omega_q \sqrt{1 - A_q}} e^{iqr_j}(\tilde{b}_q - \tilde{b}^\dagger_{-q})n_{j\sigma}. \tag{B4}$$

Applying it to the Hamiltonian and switching on the drive we obtain, *cf.* equation (8),

$$H = -\sum_{ij\sigma} J_{ij}c^\dagger_{i\sigma}c_{j\sigma} + \sum_{ij\sigma\sigma'} U_{ij}n_{i\sigma}n_{j\sigma'} + \sum_k P^R_k P^R_{-k} + \omega_k^2(1 - A_k - A_k \cos 2\Omega t)Q^R_k Q^R_{-k}. \tag{B5}$$

with dressed tunneling matrix element $J_{ij} = J_0 e^{-\frac{1}{\sqrt{V}}\sum_k \frac{g_k}{\omega_k(1 - A_k)^{3/4}}(e^{ikr_i} - e^{ikr_j})(b_k - b^\dagger_{-k})}$ and attractive electron-electron interaction $U_{ij} = -\frac{1}{V}\sum_k e^{-ik(r_j - r_i)}\frac{g_k^2}{\omega_k \sqrt{1 - A_k}}$.

2. Rotating phonon frame

We construct a unitary transformation to remove the phonon driving following Ref. [48]. We introduce the undriven and driven phonon Hamiltonian, respectively, as

$$H_0 = P_q P_{-q} + \omega_q^2 Q_q Q_{-q} = \omega_q(b^\dagger_q b_q + b_{-q} b^\dagger_{-q}) \tag{B6a}$$

$$H_1 = P_q P_{-q} + \omega_q^2 \Omega_t^2 Q_q Q_{-q} = \frac{1}{2}(\Omega_t^2 + 1)\omega_q(b^\dagger_q b_q + b_{-q} b^\dagger_{-q}) + \frac{1}{2}(\Omega_t^2 - 1)\omega_q(b^\dagger_q b^\dagger_{-q} + b_q b_{-q}). \tag{B6b}$$

Applying the unitary transformation, we find

$$i\frac{d}{dt}W |\psi_0\rangle = i\frac{dW}{dt}|\psi_0\rangle + Wi\frac{d}{dt}|\psi_0\rangle = i\frac{dW}{dt}|\psi_0\rangle + WH_0 |\psi_0\rangle = H_1 W |\psi_0\rangle \tag{B7}$$

yielding

$$i\frac{dW}{dt}W^\dagger + WH_0W^\dagger = H_1. \tag{B8}$$

Relation (10) from the main text is obtained by multiplying this equation from left by W and from right by $W^\dagger$ and by identifying $H_0 = H_{0,\text{ph}}$ and $H_1 = H_{\text{ph},0} + H_{\text{drv}}$.

Our goal is to construct a mapping of the quantum problem onto a classical Mathieu equation which determines the transformation W [48] uniquely. To this end, we introduce the Ansatz

$$W(t) = e^{\xi e^{-2i\omega_q t}K_+ - \xi^* e^{2i\omega_q t}K_-} e^{-2iK_0\phi}, \tag{B9}$$

where

$$K_0 = \frac{1}{2}(b^\dagger_q b_q + b_{-q}b^\dagger_{-q}), \qquad K_+ = b^\dagger_q b^\dagger_{-q}, \qquad K_- = b_q b_{-q}, \tag{B10}$$

which obey SU(2) algebra $[K^-, K^+] = 2K_0$, $[K^0, K^\pm] = \pm K^\pm$. The time dependent factors in equation (B9) are chosen such that $b_q e^{i\omega_q t} = \hat{b}_q(t)$ are invariants of the undriven problem H_0, which are defined by requiring that they commute with the corresponding action, i.e., $[\hat{b}_q(t), i\partial_t - H_0] = 0$. For a given invariant $\hat{b}_q(t)$, $\hat{b}_q(t)|\psi\rangle$ remains an eigenstate of H_0 provided $|\psi\rangle$ is an eigenstate, since $0 = [\hat{b}_q(t), i\partial_t - H_0]|\psi\rangle = (i\partial_t - H_0)\hat{b}_q(t)|\psi\rangle$. We furthermore introduce the invariants of the driven problem as

$$[\hat{a}_q(t), i\partial_t - H_1] = 0, \tag{B11}$$
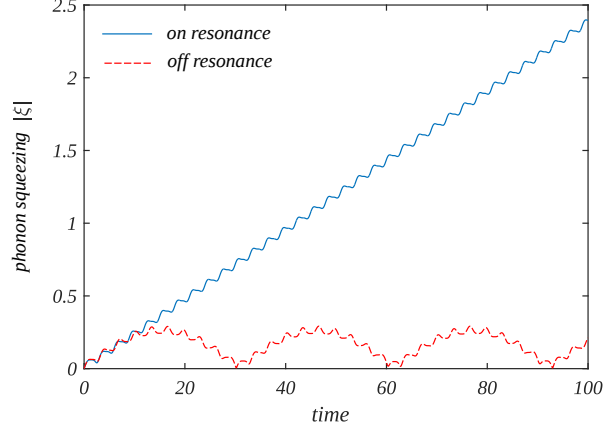
FIG. 5. **Mathieu equation**. Numerical solution of the Mathieu equation at parametric resonance ($A = 0.1$, $\Omega = \omega\sqrt{1-A}$), blue solid line, and off resonance ($A = 0.1$, $\Omega = 0.9\omega\sqrt{1-A}$), red dashed line. On resonance the phonon squeezing $|\xi|$ increases linearly in time, while off resonance it oscillates around a finite mean value.

which will be generated by the unitary transformation $\hat{a}_q(t) = W b_q(t) W^\dagger$. By differentiation and subsequent integration we obtain for the invariants

$$\hat{a}_q(t) = W b_q(t) W^\dagger = e^{i\phi}(\cosh|\xi| b_q e^{i\omega_q t} - \frac{\xi e^{-i\omega_q t}}{|\xi|}\sinh|\xi| b_{-q}^\dagger) \equiv \chi(t) b_q + \lambda^*(t) b_{-q}^\dagger \tag{B12a}$$

$$\hat{a}_{-q}^\dagger(t) = W b_{-q}^\dagger(t) W^\dagger = e^{-i\phi}(\cosh|\xi| b_{-q}^\dagger e^{-i\omega_q t} - \frac{\xi^* e^{i\omega_q t}}{|\xi|}\sinh|\xi| b_q) \equiv \chi^*(t) b_{-q}^\dagger + \lambda(t) b_q. \tag{B12b}$$

We do not explicitly write the q dependence in χ and λ, as these functions are symmetric in q, i.e., $\chi_q = \chi_{-q}$.

Next, we compute the invariants $i\partial_t \hat{a}_q(t) = [H, \hat{a}_q(t)]$, (B11), using relations (B12)

$$\frac{d\chi}{dt} = i\frac{\omega_q}{2}(\Omega_t^2 + 1)\chi - i\frac{\omega_q}{2}(\Omega_t^2 - 1)\lambda^* \tag{B13a}$$

$$\frac{d\lambda^*}{dt} = -i\frac{\omega_q}{2}(\Omega_t^2 + 1)\lambda^* + i\frac{\omega_q}{2}(\Omega_t^2 - 1)\chi. \tag{B13b}$$

We transform $\alpha = \chi - \lambda^*$, $\beta = \chi + \lambda^*$ which yields the Mathieu equation

$$\frac{d^2\alpha}{dt^2} + \omega_q^2 \Omega_t^2 \alpha = 0 \qquad \frac{d\alpha}{dt} = i\omega_q \beta. \tag{B14}$$

From the initial conditions that require $\chi(0) = 1$, $\lambda(0) = 0$, we find

$$\alpha(0) = 1, \qquad \dot{\alpha}(0) = i\omega_q. \tag{B15}$$

Using the definition of χ, λ we find the relations between $\xi(t), \phi(t)$ from the unitary transformation equation (B9) and the parameters of the Mathieu equation [47]

$$\cosh|\xi| e^{i\phi} = \frac{e^{-i\omega t}}{2}(\alpha - \frac{i\dot{\alpha}}{\omega_q}) \tag{B16a}$$

$$\sinh|\xi| \frac{\xi}{|\xi|} e^{i\phi} = \frac{e^{i\omega t}}{2}(\alpha + \frac{i\dot{\alpha}}{\omega_q}). \tag{B16b}$$

Plugging in the driving from equation (B5), we find $\Omega_t^2 = (1 - A_q - A_q \cos 2\Omega t)$. Even though the Mathieu equation can not be solved analytically, for this form of the driving its solution is well understood, as it realizes the parametric oscillator [47], which displays a parametric resonance when $\Omega = \omega\sqrt{1-A}$. On resonance the phonon squeezing $|\xi|$ increases linearly in time while off resonance it oscillates around a mean value, Fig. 5.

Now we turn again to the electron-phonon problem. Using the unitary transformation W, we remove the driving in equation (B5). Following equation (10) we have to transform the phonon operators in the dressed kinetic energy according to $W^\dagger \cdot W$

$$W^\dagger b_q W = \cosh|\xi|e^{i\phi}b_q + \frac{\xi e^{-2i\omega_q t}}{|\xi|}\sinh|\xi|e^{-i\phi}b^\dagger_{-q} \tag{B17a}$$

$$W^\dagger b^\dagger_{-q} W = \cosh|\xi|e^{-i\phi}b^\dagger_{-q} + \frac{\xi^* e^{2i\omega_q t}}{|\xi|}\sinh|\xi|e^{i\phi}b_q. \tag{B17b}$$

The initial phonon vacuum remains the ground state in the rotating frame. Hence, we take the phonon vacuum expectation value of the dressed kinetic energy and find

$$J(t) = -J_0 e^{-\frac{1}{2V}\sum_q (2-2\cos q(r_i-r_j))\frac{g_q^2}{\omega_q^2(1-A_k)^{3/2}}|\alpha_q|^2}, \tag{B18}$$

where $\alpha_q = (\cosh|\xi| - \frac{\xi^* e^{2i\omega_q t}}{|\xi|}\sinh|\xi|)e^{i\phi}$, which upon time averaging yields equation (3).

3. Rescaling of time

It is convenient to transform the time evolution from the kinetic energy to the interaction energy. Once, we evaluated the phonon dynamics, equation (B18), we obtain the effective electron Hamiltonian of the form

$$H(t) = J(t)\hat{H}_T - U\hat{H}_U, \tag{B19}$$

where we used $\hat{H}_T$ and $\hat{H}_U$ as short hand notation for the kinetic energy and the interaction energy, respectively, and $J(t)$ is the time dependent hopping matrix element. We introduce $J(t) = J_{eq}e^{-\zeta}j(t)$ where $j(t)$ is an oscillating function with mean value one. In order to move the time dependence from the kinetic energy to the interaction energy, we consider

$$\int_0^t H(t)dt = \int_0^t \tilde{H}(t)\underbrace{j(t)dt}_{dt'} = \int_0^{t'} \tilde{H}(f(t'))dt' \tag{B20}$$

where

$$\tilde{H}(\tau) = J_{eq}e^{-\zeta}\hat{H}_T - \frac{U}{j(\tau)}\hat{H}_U \tag{B21}$$

and

$$t' = \int_0^{t'} dt' = \int_0^t j(t)dt = f^{-1}(t). \tag{B22}$$

The inverse of this equation cannot be calculated analytically, however, for an oscillating function with amplitude small compared to the mean of $j(t)$ follows that $t \sim t'$ which holds because we chose $j(t)$ to oscillate around one. Thus we can directly transform the time dependent part from $J(t)$ to the interaction and arrive at

$$\tilde{H}(t) = J_{eq}e^{-\zeta}\hat{H}_T - \frac{U}{j(t)}\hat{H}_U. \tag{B23}$$

As we show in the next section, the oscillations in the interaction can be well described by a single harmonic.

4. Time dependence of the microscopic parameters

For a dispersive phonon with spread $\Delta\omega$ the time evolution of $U/J(t)$ typically oscillates at driving frequency Ω which is a common oscillation frequency for the phonon modes at all wave vectors. We approximate the oscillations of $U/J(t)$ with a single harmonic of frequency Ω and strength $\mathcal{A}$, see Fig. 6. In case of strongly off-resonant driving, the interaction oscillates around its equilibrium value, while near the parametric resonance on average it is enhanced, as a result of the polaronic suppression of the bandwidth $J_{eq}e^{-\zeta}$. The mean suppressed bandwidth $J_{eq}e^{-\zeta}$ and strength $\mathcal{A}$ of the oscillations in $U/J(t)$ are extracted numerically, *cf.* Fig. 7.
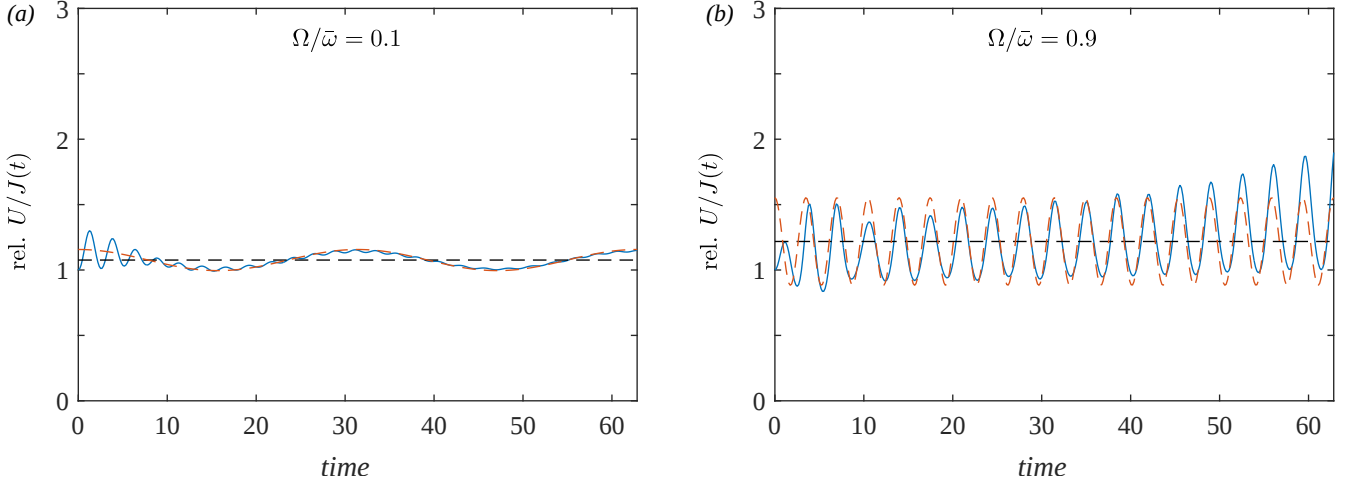
FIG. 6. **Relative strength of the oscillations in the microscopic parameters**. We show the time dependence of $U/J(t)$ relatively to the undriven system for $\bar{\omega} = U = W/8$, $\Delta\omega = 0.2\bar{\omega}$, $A = 0.1$, (a) off resonance $\Omega/\bar{\omega} = 0.1$ and (b) near the parametric resonance $\Omega/\bar{\omega} = 0.9$ (blue solid line). Initially oscillations at multiple frequencies appear, however, all oscillations except for the driving frequency are washed out in time because for a dispersive phonon the only common frequency of all modes is the driving frequency. Oscillations with Ω are indicated by the red dashed line which we choose to approximate the dynamics of the microscopic parameters. The time average of $U/J(t)$, black dashed line, is enhanced near resonance and with increasing driving strength.
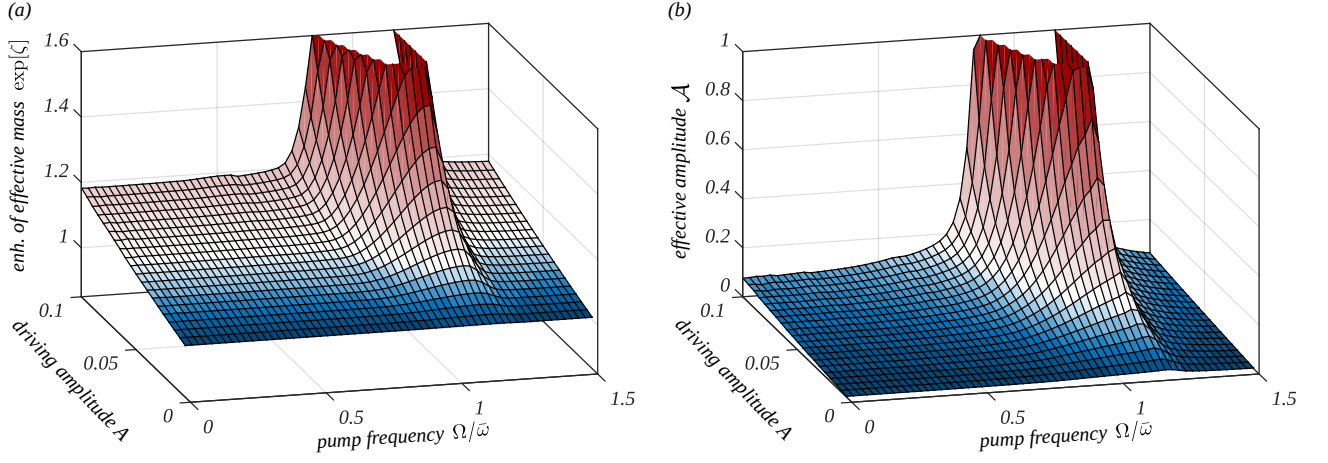
FIG. 7. **Relative enhancement of the effective mass in the driven system compared to the undriven one and the amplitude of coherent oscillations.** The data is shown for linearly dispersing phonons $\bar{\omega} = U = W/8$, and $\Delta\omega = 0.2\bar{\omega}$. Near $\Omega/\bar{\omega} \sim 1$ we find a strong enhancement of (a) the effective mass $\exp[\zeta]$ and (b) the effective amplitude $\mathcal{A}$ due to the efficient phonon squeezing. Furthermore, a weaker enhancement is observed at the higher order resonances where $\Omega/\bar{\omega} \sim 1/n$ with n being an integer. In addition to the enhancement of the effective mass near the parametric resonance, it generically increases with increasing driving amplitude A due to the softening of the phonon modes.

5. Floquet Fermi's Golden Rule

The full form of the effective Hamiltonian (4) is

$$\bar{H} = -J_{\text{eq}}e^{-\zeta} \sum_{ij\sigma} e^{-\sum_k \alpha_k^*(t)\Gamma_k^* b_k^\dagger} e^{\sum_k \alpha_k(t)\Gamma_k b_k} c_{i\sigma}^\dagger c_{j\sigma} - U(1 + \mathcal{A}\cos 2\Omega t) \sum_i n_{i\uparrow} n_{i\downarrow}, \tag{B24}$$

where $\Gamma_k = -\frac{1}{\sqrt{V}}(e^{ikr_i} - e^{ikr_j})\frac{g_k}{\omega_k(1-A_k)^{3/4}}$. Taking the phonon vacuum expectation value of equation (B24), we obtain the first two terms of equation (4). The electron-phonon scattering term, represented by the last term in equation (4) is given by $\hat{H}_{\text{el-ph scatt.}} = -J_{\text{eq}}e^{-\zeta} \sum_{ij\sigma}(e^{-\sum_k \alpha_k^*(t)\Gamma_k^* b_k^\dagger} e^{\sum_k \alpha_k(t)\Gamma_k b_k} - 1)c_{i\sigma}^\dagger c_{j\sigma}$ which as discussed vanishes upon taking

the phonon vacuum expectation value. Using a Floquet Fermi's Golden Rule analysis we estimate the Cooper pair-breaking rate which originates from both (i) phonon fluctuations in the kinetic energy and (ii) modulation of the effective electron-electron interactions.

    a. Phonon Fluctuations. Fluctuations around the phonon vacuum require energy. This energy can be borrowed from the time dependence of the drive. Expanding the exponentials of the electron phonon scattering term $\hat{H}_{\text{el-ph scatt.}}$ to first order, we obtain

$$\hat{H}_{\text{el-ph scatt.}} \sim -J_{\text{eq}}e^{-\zeta}\frac{1}{\sqrt{V}}\sum_{kq\sigma}\frac{2g_q}{\omega_q(1-A_q)^{3/4}}[\sum_d \cos k_d - \cos(k_d - q_d)](\alpha_q(t)b_q - \alpha^*_{-q}(t)b^\dagger_{-q})c^\dagger_{k\sigma}c_{k-q\sigma}$$

$$= \frac{1}{V}\sum_{kq\sigma}[\mathcal{F}_{qk}\alpha_q(t)b_q - \mathcal{F}^*_{qk}\alpha^*_q(t)b^\dagger_{-q}]c^\dagger_{k\sigma}c_{k-q\sigma} \tag{B25}$$

with

$$\mathcal{F}_{kq} = -2J_{\text{eq}}e^{-\zeta}[\sum_d \cos k_d - \cos(k_d - q_d)]\frac{g_q}{\omega_q(1-A_q)^{3/4}}. \tag{B26}$$

Higher order terms in the series expansion of the exponentials correspond to multi-phonon processes which are energetically suppressed.

    The finite lifetime of quasiparticles at the Fermi energy can be calculated from the imaginary part of the retarded phonon-fluctuation self energy

$$\frac{1}{\tau_{\text{ph}}} = \text{Im}\,\Sigma^{\text{ph},+}_{k_F}. \tag{B27}$$

To leading order the corresponding greater and lesser components are

$$\Sigma^{\text{ph},\gtrless}_k(t_1,t_2) = \quad\text{}\quad = \frac{i}{V}\sum_q |\mathcal{F}_{kq}|^2 \alpha_q(t_1)\alpha^*_q(t_2)G^{\gtrless}_{k-q}(t_1,t_2)D^{\gtrless}_q(t_1,t_2). \tag{B28}$$

Here, $G^{\gtrless}_k(t_1,t_2)$ is the bare electron and $D^{\gtrless}_q(t_1,t_2)$ the bare phonon propagators, which are functions of the time difference as the unperturbed Hamiltonian is static. Thus, in Fourier space they are given by

$$G^>_k(\omega) \approx -2\pi i\delta(\omega - \epsilon_k + \mu)[1 - n_k],$$
$$G^<_k(\omega) \approx +2\pi i\delta(\omega - \epsilon_k + \mu)n_k,$$
$$D^>_q(\omega) \approx -i\pi\delta(\omega - \omega_q),$$
$$D^<_q(\omega) \approx -i\pi\delta(\omega + \omega_q),$$

where we considered the phonons to be in the vacuum state and thus neglected their distribution functions in $D^>$ and $D^<$. The self-energy contains the drive $\alpha_q(t)$ and therefore is a fully non-equilibrium object which is a function of two times, equation (B28). We rewrite the self-energy using the average time $T = \frac{1}{2}(t_1 + t_2)$ and the time difference $t = t_1 - t_2$

$$\Sigma^{\text{ph},\gtrless}_k(t,T) = \frac{i}{V}\sum_q |\mathcal{F}_{kq}|^2 \alpha_q(T+t/2)\alpha^*_q(T-t/2)G^{\gtrless}_{k-q}(t)D^{\gtrless}_q(t). \tag{B29}$$

In order to estimate a quasi-particle lifetime, we integrate over the "slow" timescale T which yields for the effective coupling $|\bar{\alpha}_q(t)|^2 = \frac{\Omega}{\pi}\int_0^{\frac{\pi}{\Omega}}dT\,\alpha_q(T+t/2)\alpha^*_q(T-t/2)$. The effective coupling $|\bar{\alpha}_q(t)|^2$, distinguished from the bare coupling by the bar, is only a function of the time difference t. From a Fourier transform we obtain its Floquet components $|\bar{\alpha}_{qn}|^2$, where n ranges from $-\infty$ to ∞. We calculate the retarded self-energy $\Sigma^+_{\text{ph},k}$ using

$$\Sigma^{\text{ph},+}_k(\omega) = i\int \frac{d\omega'}{2\pi}\frac{\Sigma^{\text{ph},>}_k(\omega') - \Sigma^{\text{ph},<}_k(\omega')}{\omega - \omega' + i0^+}, \tag{B30}$$

where ω is the conjugate variable to the time difference t, and find for the lifetime at the Fermi surface

$$\frac{1}{\tau_{\text{ph}}} = \frac{\pi}{2V}\sum_{qn}|\mathcal{F}_{qk_F}|^2|\bar{\alpha}_{qn}|^2\{(1 - n_{k_F-q})\delta(2n\Omega - E_{k_F-q} - \omega) + n_{k_F-q}\delta(2n\Omega - E_{k_F-q} + \omega)\}. \tag{B31}$$

In order to obtain a semi-analytical estimate for the pair breaking rate, we neglect the weak wavevector dependence of $g_q/\omega_q(1-A_q)^{3/4}$ and replace them by their mean. We replace wavevector summations by integrals over energies with a constant density of states, yielding

$$\frac{1}{\tau_{\text{ph}}} = \frac{\pi}{2}\sum_{n>0}\frac{e^{\zeta}}{8J_{\text{eq}}}\frac{\bar{g}^2}{\bar{\omega}^2(1-A)^{3/2}}(2n\Omega-\bar{\omega})^2\Theta(2n\Omega-\bar{\omega})\{\alpha_n\Theta(|E_F+2n\Omega-\bar{\omega}|-W)+\alpha_{-n}\Theta(|E_F-2n\Omega+\bar{\omega}|-W)\}, \quad \text{(B32)}$$

where $W = 4J_{\text{eq}}e^{-\zeta}$ is half of the electronic bandwidth.

b. Modulated interactions. The temporal modulation of the effective electron-electron interaction leads to another source for decreasing the quasiparticle lifetime. Similarly as in the case of phonon fluctuations, we estimate the interaction decay rate by computing the imaginary part of the leading order self-energy contribution

$$\Sigma_k^{\text{int},\gtrless}(t_1,t_2) = \quad \diamondsuit \quad = \frac{1}{V^2}\sum_{ql}U^2(1+\mathcal{A}\cos 2\Omega t_1)(1+\mathcal{A}\cos 2\Omega t_2)G_{k+l-q}^{\gtrless}(t_1,t_2)G_q^{\gtrless}(t_1,t_2)G_l^{\lessgtr}(t_2,t_1). \quad \text{(B33)}$$

Performing a Floquet Fermi's Golden Rule analysis, we first integrate over the "slow" timescale T to obtain an effective coupling as a function of the time difference t and then compute the Floquet components of the coupling. Plugging this into the expression for the retarded self-energy and taking the imaginary part, we obtain the decay rate

$$\frac{1}{\tau_{\text{int}}} = \frac{U^2\mathcal{A}^2}{4V^2}\sum_{ql}[(1-n_{k_F+l-q})(1-n_q)n_l+n_{k_F+l-q}n_q(1-n_l)][\delta(2\Omega-(E_{k_F+q-l}+E_q-E_l))+\delta(2\Omega+(E_{k_F+q-l}+E_q-E_l))].$$
$$\text{(B34)}$$

We evaluate both quasiparticle decay rates numerically, *cf.* Fig. 3. The total pair-breaking rate $1/\tau = 1/\tau_{\text{ph}}+1/\tau_{\text{int}}$, which we consider as an imaginary self-energy correction in the Floquet BCS equations, is in a wide parameter range much smaller than the Cooper pair formation rate and thus only slightly shifts the transition temperature to lower values.

Appendix C: Floquet BCS approach

We first evaluate the equations of motion for $c_{k\uparrow}^\dagger c_{-k\downarrow}^\dagger$ from the rescaled Hamiltonian equation (4) taking into account the Cooper pair breaking rate $1/\tau$, computed in Sec. B 5, as an imaginary self-energy correction

$$\frac{d}{dt}c_{k\uparrow}^\dagger c_{-k\downarrow}^\dagger = 2i(\epsilon_k+i/\tau-\mu)c_{k\uparrow}^\dagger c_{-k\downarrow}^\dagger - i\frac{U(1+\mathcal{A}\cos 2\Omega t)}{V}\sum_{mq}c_{m\uparrow}^\dagger c_{q\downarrow}^\dagger(c_{m+q-k\downarrow}c_{-k\downarrow}^\dagger - c_{k\uparrow}^\dagger c_{m+q+k\uparrow}) \quad \text{(C1)}$$

and factorize the quartic term using a mean-field decoupling

$$\frac{d}{dt}\langle c_{k\uparrow}^\dagger c_{-k\downarrow}^\dagger\rangle = 2i(\epsilon_k+i/\tau-\mu)\langle c_{k\uparrow}^\dagger c_{-k\downarrow}^\dagger\rangle - i\frac{U(1+\mathcal{A}\cos 2\Omega t)}{V}\sum_q\langle c_{k\uparrow}^\dagger c_{-k\downarrow}^\dagger\rangle(n_{q\uparrow}+n_{q\downarrow})+\langle c_{q\uparrow}^\dagger c_{-q\downarrow}^\dagger\rangle(1-n_{k\uparrow}-n_{k\downarrow}). \quad \text{(C2)}$$

Using spin symmetry and defining $2\rho = \frac{1}{V}\sum_q(n_{q\uparrow}+n_{q\downarrow})$ we obtain

$$\frac{d}{dt}\langle c_{k\uparrow}^\dagger c_{-k\downarrow}^\dagger\rangle = 2i(\epsilon_k+i/\tau-\mu-U(1+\mathcal{A}\cos 2\Omega t)\rho)\langle c_{k\uparrow}^\dagger c_{-k\downarrow}^\dagger\rangle - iU(1+\mathcal{A}\cos 2\Omega t)(1-2n_k)\frac{1}{V}\sum_q\langle c_{q\uparrow}^\dagger c_{-q\downarrow}^\dagger\rangle. \quad \text{(C3)}$$

Next, we remove the term $2iU\rho\mathcal{A}\cos 2\Omega t\langle c_k^\dagger c_{-k}^\dagger\rangle$ by an appropriate unitary transformation of the form

$$\langle c_{k\uparrow}^\dagger c_{-k\downarrow}^\dagger\rangle = a_k^*\exp[-i\frac{U\rho\mathcal{A}}{\Omega}\sin 2\Omega t] \quad \text{(C4)}$$

which gives:

$$\frac{d}{dt}a_k^* = 2i(\epsilon_k+i/\tau-\mu-U\rho)a_k^* - iU(1+\cos 2\Omega t)(1-2n_k)\frac{1}{V}\sum_q a_q^*. \quad \text{(C5)}$$

Using the Floquet Ansatz

$$a_k^*(t) = e^{iEt}\sum_n a_{kn}^* e^{i2n\Omega t} \quad \text{(C6)}$$

we obtain

$$[E + 2n\Omega - 2(\epsilon_k + i/\tau - \mu - U\rho)]a_{kn}^* = -(1 - 2n_k)\frac{U}{V}\left[\sum_q a_{qn}^* + \frac{\mathcal{A}}{2}\sum_q (a_{qn+1}^* + a_{qn-1}^*)\right]. \tag{C7}$$

Dividing by $E + 2n\Omega - 2(\epsilon_k + i/\tau - \mu - U\rho)$, and summing over k, we find the Floquet BCS gap equation:

$$\frac{1}{V}\sum_k a_{kn}^* = -\underbrace{\frac{1}{V}\sum_k \frac{1 - 2n_k}{E + 2n\Omega - 2(\epsilon_k + i/\tau - \mu - U\rho)}}_{=F_n}\frac{U}{V}\left[\sum_q a_{qn}^* + \frac{\mathcal{A}}{2}\sum_q (a_{qn+1}^* + a_{qn-1}^*)\right]. \tag{C8}$$

Defining the gap $\Delta_n = \frac{U}{V}\sum_k a_{kn}^*$, we obtain the simple system of equations

$$(U^{-1} + F_n)\Delta_n + \frac{\mathcal{A}}{2}F_n(\Delta_{n-1} + \Delta_{n+1}) = 0. \tag{C9}$$

The fact that we used a single harmonic to describe the time evolution of $U(t)$ reflects in the gap equation having only a single side band. More complicated functions would lead to further side bands which would give quantitative differences but our conclusions will not be altered on the qualitative level. The BCS Floquet equations have a nontrivial solution, when the determinant is zero, which we determine by scanning E in the complex plane. The Cooper pair formation rate is characterized by the imaginary part of E.